

LANE 2010

## THz Imaging and Spectroscopy using Intense THz Sources at the Advanced Laser Light Source

T. Ozaki<sup>a,\*</sup>, F. Blanchard<sup>a</sup>, G. Sharma<sup>a</sup>, L. Razzari<sup>a,b</sup>, X. Ropagnol<sup>a</sup>, F. Vidal<sup>a</sup>,  
R. Morandotti<sup>a</sup>, J.-C. Kieffer<sup>a</sup>, Matt Reid<sup>c</sup>, and F. Hegmann<sup>d</sup>

<sup>a</sup>*Institut national de la recherche scientifique, Centre Énergie, Matériaux, Télécommunications,  
1650 boul. Lionel-Boulet, Varennes, Québec J3X 1S2 Canada*

<sup>b</sup>*Dipartimento di Elettronica, Università di Pavia, via Ferrata 1, 27100 Pavia, Italy*

<sup>c</sup>*Department of Physics, University of Northern British Columbia, Prince George, British Columbia V2N 4Z9, Canada*

<sup>d</sup>*Department of Physics, University of Alberta, Edmonton, Alberta T6G 2G7, Canada*

### Invited Paper

---

#### Abstract

There has recently been a surge of new laser-based techniques for generating intense, few-cycle terahertz (THz) pulses, thus opening new applications, such as studying the nonlinear optical properties of various materials at THz frequencies. Simultaneously, innovative solutions for broadband THz detection were found, allowing one to sense matter in the THz range with high temporal resolution. In this paper, we will review the properties and characteristics of recently developed intense THz sources, with a particular eye on their potential applications, such as ultrafast THz nonlinear spectroscopy.

© 2010 Published by Elsevier B.V. Open access under [CC BY-NC-ND license](https://creativecommons.org/licenses/by-nc-nd/4.0/).

Keywords: THz-Spectroscopy; Large Aperture Optical Rectification; Pulse Front Phase Technique

---

#### 1. Introduction

Terahertz (THz) radiation covers the electromagnetic spectrum from 300 GHz to 20 THz, bridging the gap between microwaves and infrared light. THz waves have the unique ability to penetrate various materials, including non-metallic compounds (papers, plastics), organics, gases and liquids, thus being a powerful tool for spectroscopic sensing [1]. Since THz waves may be generated and detected using ultrashort laser pulses, coherent time-domain THz spectroscopy with sub-picosecond temporal resolution now provide unprecedented insights into the nature of molecular vibrations, carrier dynamics in semiconductors, and protein kinetics [2–4]. Since the first demonstration of coherent THz detection by Auston *et al.* [5] in 1983, there has been many works on developing new and improved generation and detection techniques, as well as on the application of THz radiation, especially in spectroscopy [6,7] and imaging [8,9].

---

\* Corresponding author. Tel.: +1-450-929-8258.  
E-mail address: [ozaki@emt.inrs.ca](mailto:ozaki@emt.inrs.ca).

Recently, intense THz sources in the micro-joule range have been successfully developed, which has been used to open new possibilities in THz science, such as probing the ultrafast nonlinear optical properties of materials in the THz frequency region [10–15]. We note that for developing nonlinear THz optics, synchrotron sources have already been available for some time, which can generate intense single-cycle THz pulses with as many as few tens of micro-joule energy per pulse. However these sources still suffer from a significant time jitter, which in turn makes coherent detection difficult [16]. In this paper, we will summarize some of the recent developments in the generation and application of intense THz radiation using both optical rectification methods. In particular, we will summarize the work carried out at the Advanced Laser Light Source (ALLS), located at the Institut National de la Recherche Scientifique, (INRS) near Montreal, Canada.

## 2. Large Aperture Optical Rectification

### 2.1. Experimental setup

Experiments were performed at the ALLS laboratory, which is an international laser user facility equipped with intense Ti:sapphire lasers with different energy and repetition rates. A new beam line at ALLS has been configured to generate intense THz sources [17]. This THz source is pumped by a laser beam line that delivers 800-nm light with energies as high as 70 mJ (after the vacuum compressor), 30 fs temporal duration and at a repetition rate of 100 Hz. The experimental setup shown in Fig. 1 includes three main parts: a THz generation chamber held under vacuum ( $<10^{-6}$  torr), an 800-nm probe beam line propagating in air, and a dry-nitrogen-purged section. For the THz emitters, we have the choice of either a 0.5-mm-thick or a 1.0-mm-thick large aperture (110) ZnTe single crystal wafer, both having a diameter of 75 mm (Nikko Materials). To minimize saturation effects and to avoid damage of the crystal surface, the 800-nm beam was spatially expanded to about 40 mm FWHM (or 36 cm<sup>2</sup> for full-width at  $1/e^2$  maximum) at the surface of the ZnTe emitter. In addition, the ZnTe crystal was rotated in its mount to maximize the THz emission via optical rectification [18]. Any remaining 800-nm light transmitted through the ZnTe wafer was blocked using two black polyethylene absorbers, which were transparent to the THz radiation. The emitted THz pulse is first focused by a gold-coated off-axis parabolic mirror (100 mm clear aperture, 150 mm focal length), which is placed in vacuum. The THz beam passes through a 2-mm-thick polypropylene window, and is then re-collimated by another identical off-axis parabolic mirror outside the vacuum chamber. To facilitate steering of the THz beam, the beam size was reduced by 2 times using a 50 mm clear aperture, 75 mm focal length off-axis parabolic mirror, thereby preserving the numerical aperture of the THz optics. A mechanical chopper positioned at the first focus modulates the THz beam for lock-in amplification. Two 100 mm diameter wire-grid polarizers were also installed to control the intensity and the polarization of the THz beam and were primarily used for characterizing the linearity of the detector.

We detected the THz pulse waveform using free-space electro-optic (EO) sampling in a second (110) ZnTe crystal with a thickness of 20  $\mu\text{m}$ , mounted on top of a 0.5 mm thick (100) backing crystal. A lock-in amplifier connected to the output of the balanced photodiodes and referenced to the chopper was used to acquire the THz waveforms. The THz energy was measured using a pyroelectric detector (Coherent-Moletron) with a specified sensitivity of 2.624 V/J at 1.06  $\mu\text{m}$ , which we previously calibrated at THz frequencies using a second pyroelectric detector from Microtech Instruments [17]. To further characterize the THz beam, a BaSrTiO<sub>3</sub> (BST) pyroelectric infrared camera (Electrophysics, model PV320) was used to image the THz beam at the focus. This camera operates with an internal 10 Hz chopper and consists of a 320  $\times$  240 pixel imaging array with a pixel spacing of 48.5  $\mu\text{m}$ .

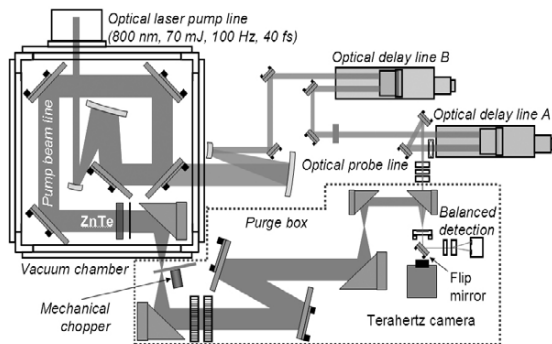


Fig. 1. Schematics of the experimental setup for intense THz radiation waves based on optical rectification in a large aperture ZnTe crystal.

### 2.2. THz energy

We have measured the azimuthal angle ( $\theta$ ) dependence of the emitted THz energy. The emission of THz radiation as a function of  $\theta$  is expected to be proportional to  $\sin^2(2\theta) + \sin^4(\theta)$ . We find excellent agreement between theory and experimental data, proving that the optical rectification process is indeed responsible for the emitted THz energy. An interesting result obtained using the large aperture ZnTe source is the scaling of the THz energy versus laser pump energy, shown in Fig. 2. The pump beam irradiating the ZnTe crystal has a fluence ranging from  $28 \mu\text{J cm}^{-2}$  (1 mJ) to  $1.33 \text{ mJ cm}^{-2}$  (48 mJ) with a Gaussian shape and a beam size of 40 mm FWHM, equivalent to a total area of  $36 \text{ cm}^2$ . At the maximum pump energy of 48 mJ the THz pulse energy is as high as 1.5  $\mu\text{J}$ , corresponding to an energy conversion efficiency of  $3.1 \times 10^{-5}$  and an average THz power of 150  $\mu\text{W}$  (for 100 Hz repetition rate). To the best of our knowledge, this result is still the highest THz energy reported from an optical rectification process in a ZnTe crystal.

The pump fluence used in our experiment are typically well above the saturation fluence of  $50 \mu\text{J cm}^{-2}$  [19]. Therefore, we do not expect to record a quadratic increase in the THz pulse energy as a function of the 800 nm pump energy over the entire intensity range. Instead, we see a slightly super-linear increase of the THz pulse energy as a function of the excitation pulse energy, which is consistent with the data shown by Löffler *et al.* [19] above the saturation fluence (where two-photon absorption effects become significant). Even if locally the beam experiences complete saturation at the center of the beam, the THz emission continues to grow at the (lower intensity) wings, which in turn may contribute to the behavior shown in Fig. 2. A possible explanation for the higher efficiency ( $3.1 \times 10^{-5}$ ) obtained in our case compared with that reported in Ref. [19] may be due to the lower repetition rate of our laser source (100 Hz instead of 1 kHz). Our lower repetition rate may give residual free carriers enough time to recombine between subsequent pulses, thereby keeping the background free carrier concentration much lower than for higher repetition rates.

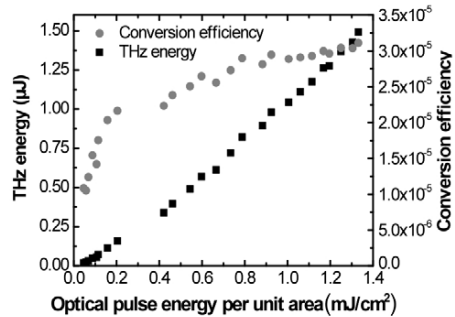


Fig. 2. THz pulse energy emitted from the large-aperture ZnTe source as a function of the incident 800 nm laser pulse energy per unit area. The corresponding energy conversion efficiency is also shown.

### 2.3. THz electric field

As mentioned previously, two ZnTe emitters were used for generating THz waves (either a 0.5-mm-thick or a 1.0-mm-thick (110) ZnTe single crystal wafer, both with a 75 mm diameter). In Fig. 3(a), we show the waveforms of the THz pulses generated by the 0.5-mm-thick and the 1.0-mm-thick (110) ZnTe crystals. As one can expect, a broader frequency content is obtained when the thinner ZnTe crystal is used to emit THz radiation. Note that the absence of frequency content above 3 THz is mainly due to the presence of phonon absorption lines in the ZnTe crystal [20].

For full evaluation of the source, we imaged the THz beam at the focus using a pyroelectric infrared camera (Electrophysics, model PV320). In this way, we could evaluate easily the peak electric field using the full characteristics of the beam, specifically the energy and physical dimensions at the focus. Recently, we have been able to capture the image of the THz beam using a pyroelectric camera, thus showing the possibility of imaging high power THz beams directly and in real-

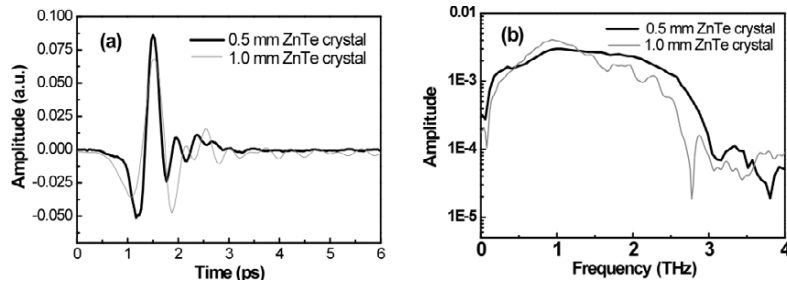


Fig. 3. (a) Pulse waveforms generated by a 0.5-mm-thick and a 1.0-mm-thick (110) ZnTe crystal. (b) Corresponding Fourier transforms of the THz pulse waveforms.

time [17]. The measured spot size is 1.6 mm at  $1/e^2$  of the intensity profile.

In our work, the evaluation of the THz electric field was carried out following a similar method as that reported in Ref. [21], that is, by using the following equation:

$$E_0 = \sqrt{\frac{\eta_0 W}{\pi w_l^2 \int g^2(t) dt}} \quad (1)$$

Here,  $E_0$  is the THz peak electric field,  $\eta_0$  is the free space impedance ( $377 \Omega$ ),  $W$  is the THz energy,  $w_l$  is the intensity beam waist, and  $g(t)$  is the temporal shape of the THz electric field (with a peak value normalized to 1), which can be easily retrieved from the EO sampling measurements. Using Eq. (1), along with the beam spot size recorded by our camera, we estimated a value of the electric field as high as  $\sim 230$  kV/cm for a 1.5  $\mu$ J THz pulse.

### 3. Tilted Pulse Front Phase Technique

#### 3.1. Background

To date, the most efficient way of generating intense THz waves in the 0.1 – 3 THz frequency range remains the recently proposed tilted pulse front technique based on the use of a LiNbO<sub>3</sub> crystal [14]. Efficient THz generation needs the group velocity of the optical pump beam  $v_{vis}^{gr}$  to match the phase velocity of the THz wave  $v_{THz}^{ph}$ , that is  $v_{vis}^{gr} = v_{THz}^{ph}$ . Many high dielectric constant materials, including LiNbO<sub>3</sub> and other ferroelectric materials offer very high EO coefficient, however the velocity matching of optical and THz waves in these crystals cannot be achieved collinearly. For these materials, the refractive index in the THz range is more than two times larger than that in the visible range. This problem is overcome by tilting the pulse front of the optical beam using a diffraction grating, as first proposed and demonstrated by Hebling *et al.* [22, 23].

The idea proposed in [22] is to tilt the pulse front of the optical pump beam relative to its phase front, as both of them are initially perpendicular to the propagation direction. By travelling in a nonlinear medium such as LiNbO<sub>3</sub>, the pump pulse propagates with a velocity  $v_{vis}^{gr}$  and the THz radiation is excited along this tilted pulse front direction. The projection of the optical beam velocity on the propagation direction of the THz beam has to be equal to the THz phase velocity, *i.e.*:

$$v_{THz}^{ph} = v_{vis}^{gr} \cdot \cos \gamma \quad (2)$$

Here,  $\gamma$  is the tilt angle introduced in the pulse front relative to the phase front. Using this technique, it is possible to equalize the two velocities by choosing an appropriate tilt angle  $\gamma$  in a material with a significantly large dielectric constant.

To tilt the pulse front of the optical beam relative to the phase front, a grating is typically used. Using simple ray optics formalism for an optical beam that is incident on the grating with an angle  $\alpha$  and is diffracted by an angle  $\beta$ , the pulse front tilt angle  $\gamma$  can be depicted.

If  $n_{opt}$  is the index of refraction of the LiNbO<sub>3</sub> crystal and  $F$  the demagnification ratio of the lens used to image the beam spot on the grating to the crystal position, the pulse front tilt angle becomes:

$$\tan \gamma = \frac{F}{n_{opt}} \frac{mN\lambda}{\cos(\beta)} \quad (3)$$

Here,  $\lambda$  is the optical pump wavelength,  $m$  is the diffraction order and  $N$  is the grating grooves number. By using Eq. (3), one can find the front tilt introduced at the crystal position. It is important to notice that the crystal has to be cut at an angle that satisfies the velocity matching condition inside the crystal.

### 3.2. Experimental setup

In our experimental setup for our THz source based on the tilted pulse front technique, installed at ALLS, we use a 1 mol% Mg-doped LiNbO<sub>3</sub> crystal. Note that doping is chosen to avoid the photorefractive effect in LiNbO<sub>3</sub> [23]. To satisfy the velocity matching condition given by Eq. (9), the crystal was cut at an angle of 63°, since the group index of the optical pulse and the phase index of the THz wave are equal to 2.26 and 4.98, respectively. The ALLS laser beam line used to pump the crystal is a Ti:sapphire laser that delivers 4 mJ pulses with 30 fs pulse duration at 1 kHz repetition rate. The 5-mm diameter beam is split into two parts using a combination of a half-wave plate and a polarizer. The horizontally polarized beam is first demagnified (by a factor of 3) using a telescope made of two lenses with focal length of 150 mm and -50 mm, respectively. This demagnification is necessary to increase the pump laser intensity at the crystal position. The demagnified, horizontally polarized beam is sent to the grating and the vertically polarized beam is used as a probe line.

Combining the grating equation with the tilt equation (Eq. 3), we calculate an angle of incidence  $\alpha = 37.31^\circ$ . The diffracted beam from the grating is imaged onto the crystal with a demagnification factor of 1.7, using an achromatic lens with a focal length of 150 mm. A half-wave plate is placed after the lens to rotate the polarization of the pump beam from horizontal to vertical, thus setting the polarization of the pump laser parallel to the LiNbO<sub>3</sub> z-axis (where the z-axis is the extraordinary axis). THz is generated from the crystal and is collected by a gold-coated off-axis parabolic mirror with a 110 mm focal length. The THz beam is focused using an off-axis parabolic mirror of 50-mm focal length on to a 0.5-mm-thick (110) ZnTe crystal. Free-space EO sampling is then used for detecting the THz signal.

### 3.3. Source characteristics

For the experimental setup illustrated above, 1.3 mJ of the total laser energy (4 mJ) was used to generate THz waves, to avoid damage on the grating surface due to the demagnified beam impinging on the grating. We recall that at the crystal position, the pump energy of the laser was 0.9 mJ, with 30 fs pulse duration, at a repetition rate of 1 kHz, and with a spot size equal to 1.7-mm diameter at  $1/e^2$ .

Figure 4 shows the recorded THz energy dependence on the pump laser energy. Conversion efficiency as high as  $6 \times 10^{-4}$ , similar to the one reported in [14], was achieved. Notice that we used the same Coherent-Molelectron pyroelectric detector used to characterize the ZnTe-based source described previously. As mentioned in Section IV-B, the THz energy extracted from an optical rectification process should scale up quadratically. From Fig. 4, it is clear that the process is partially saturated, thus resulting in a linear increase of the THz energy as function of laser pump energy. We point out once more that in the present configuration, the pump energy could not be further increased, to avoid damage of the grating. As such, we did not reach the complete saturation regime.

As we did for the large aperture ZnTe source, we measured the THz spot size using a pyroelectric infrared camera (Electrophysics, model PV320) and found a value of  $0.97 \times 0.8$  mm at the focus ( $1/e^2$  value). Substituting in Eq. (1) the pulse temporal profile recorded from the EO sampling, we evaluated a peak THz electric field at focus of  $\sim 160$  kV/cm.

## 4. Summary

In summary, we have reviewed the high intensity THz sources recently implemented at the Advanced Laser Light Source in Canada. In this paper, THz sources obtained using (i) a large aperture ZnTe crystal-based source, and (ii) a tilted pulse front technique in LiNbO<sub>3</sub> have been reported. The THz sources have been introduced in the broader context of the high intensity laser sources of the ALLS National Facility, aimed to create high intensity sources

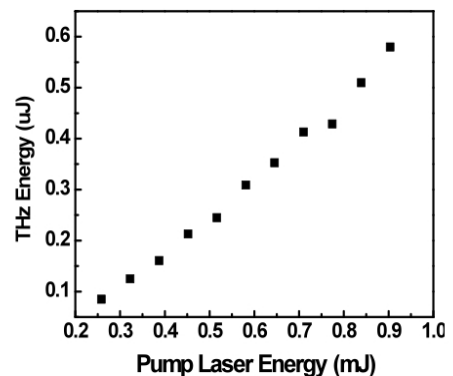


Fig 4. THz energy vs pump laser energy for the tilted pulse front configuration.

capable to cover the entire radiation spectrum from the THz to the X-rays. The results we obtained clearly show the high potential of our THz sources for nonlinear applications.

## References

- [1] D. Grischkowsky, S. Keiding, M. van Exter, and C. Fattinger, *J. Opt. Soc. Am. B* **7**, 2006 (1990).
- [2] M. C. Nuss and J. Orenstein, "Terahertz Time-Domain Spectroscopy", in *Millimeter and Submillimeter Wave Spectroscopy of Solids*, G. Grüner, ed. Springer, Berlin, (1998).
- [3] D. M. Mittleman, "Sensing with Terahertz Radiation," ed. Springer-Verlag, Berlin, (2003).
- [4] B. Ferguson and X.-C. Zhang, "Materials for terahertz science and technology" *Nature Materials* **1**, 26-33 (2002).
- [5] D. H. Auston and P.R. Smith, "Generation and detection of millimeter waves by picosecond photoconductivity," *Appl. Phys. Lett.* **43**, 631-633 (1983).
- [6] A. C. Warren, J. M. Woodall, J. L. Freeouf, D. Grischkowsky, D. T. McInturff, M. R. Melloch, and N. Otsuka, "Arsenic Precipitates and the Semi-Insulating Properties of GaAs Buffer Layers Grown by Low Temperature Molecular Beam Epitaxy," *Appl. Phys. Lett.*, **57**, 1331-1333 (1990).
- [7] J. T. Kindt, and C. A. Schmuttenmaer, "Far-infrared dielectric properties of polar liquids probed by femtosecond terahertz pulse spectroscopy" *Journal of Phys. Chemistry*, **100**, 10373-10379 (1996).
- [8] B. B. Hu and M. C. Nuss, "Imaging with terahertz waves," *Opt. Letters*, **20**, 1716-1718, (1995).
- [9] D. M. Mittleman, R. H. Jacobsen, and M. C Nuss, "T-ray imaging," *IEEE Journal of selected topics in quantum electronics*, **2**, 679-692 (1996).
- [10] P. Gaal, K. Reimann, M. Woerner, T. Elsaesser, R. Hey, and K. H. Ploog, "Nonlinear terahertz response of *n*-type GaAs," *Phys. Rev. Lett.* **96**, 187402 (2006).
- [11] Y. Shen, T. Watanabe, D. A. Arena, C.-C. Kao, J. B. Murphy, T.Y. Tsang, X. J. Wang, and G. L. Carr, "Nonlinear cross-phase modulation with intense single-cycle terahertz pulses," *Phys. Rev. Lett.* **99**, 043901 (2007).
- [12] K. Y. Kim, A. J. Taylor, J. H. Glowina, and G. Rodriguez, "Coherent control of terahertz supercontinuum generation in ultrafast laser-gas interactions," *Nature Photonics* **2**, 605 (2008).
- [13] F. Blanchard, G. Sharma, X. Ropagnol, L. Razzari, R. Morandotti and T. Ozaki, "Improved terahertz two-color plasma sources pumped by a high intensity laser beam," *Opt. Express* **17**, 6044-6052 (2009).
- [14] J. Hebling, K.-L. Yeh, M. C. Hoffmann, and K. A. Nelson, "High-power THz generation, THz nonlinear optics, and THz nonlinear spectroscopy," *IEEE J. Sel. Top. Quantum Electron.* **14**, 345-353 (2008).
- [15] S. Leinß, T. Kampfrath, K. v. Volkmann, M. Wolf, J. T. Steiner, M. Kira, S. W. Koch, A. Leitenstorfer, and R. Huber, "Terahertz coherent control of optically dark paraexcitons in Cu<sub>2</sub>O," *Phys. Rev. Lett.* **101**, 246401 (2008).
- [16] G. L. Carr, M. C. Martin, W. R. McKinney, K. Jordan, G. R. Neil, and G. P. Williams, "High-power terahertz radiation from relativistic electrons," *Nature* **420**, 153-156 (2002).
- [17] F. Blanchard, L. Razzari, H.-C. Bandulet, G. Sharma, R. Morandotti, J.-C Kieffer, T. Ozaki, M. Reid, H. F. Tiedje, H. K. Haugen, and F. A. Hegmann, "Generation of 1.5 μJ single-cycle terahertz pulses by optical rectification from a large aperture ZnTe crystal," *Opt. Express* **15**, 13212-13220 (2007).
- [18] A. Rice, Y. Jin, X. F. Ma, X.-C. Zhang, D. Bliss, J. Larkin, and M. Alexander, "Terahertz optical rectification from (110) zincblende crystals," *Appl. Phys. Lett.* **64**, 1324-1326 (1994).
- [19] T. Löffler, T. Hahn, M. Thomson, F. Jacob, and H. G. Roskos, "Large-area electro-optic ZnTe terahertz emitters," *Opt. Express* **13**, 5353 (2005).
- [20] G. Gallot, J. Zhang, R. W. McGowan, T.-I. Jeon and D. Grischkowsky, "Measurements of the THz absorption and dispersion of ZnTe and their relevance to the electro-optic detection of the THz radiation", *Appl. Phys. Lett.* **74**, 3450-3452 (1999).
- [21] M. D. Thomson, M. Kreß, T. Löffler, and H. G. Roskos, "Broadband THz emission from gas plasmas induced by femtosecond optical pulses: From fundamentals to applications," *Laser Photon. Rev.* **1**, 349–368 (2007).
- [22] J. Hebling, G. Almási, I. Z. Kozma and J. Kuhl, "Velocity matching by pulse front tilting for large area THz-pulse generation," *Optics Express* **10**, 1161-1166 (2002).
- [23] J. Hebling, A. G. Stepanov, G. A. Asi, B. Bartal, and J. Kuhl, "Tunable THz pulse generation by optical rectification of ultrashort laser pulses with tilted pulse fronts," *Appl. Phys. B* **78**, 593-599 (2004).